Thermal Spreading of MoO₃ onto Silica Supports

Silvana Braun, Lucia G. Appel,[†] Vera L. Camorim,[‡] and Martin Schmal*

NUCAT/PEQ/COPPE, Universidade Federal do Rio de Janeiro-UFRJ, Centro de Tecnologia bl.G, 68502-970, Rio de Janeiro, Brazil

The thermal spreading of MoO₃ onto silica was studied in comparison with the thermal spreading onto alumina using different characterization techniques. X-ray diffraction results showed that MoO₃ crystals were transformed into Mo amorphous species on alumina and silica supports by thermal treatment. Laser Raman spectroscopy results also evidenced the transformation of MoO₃ bulk into small Mo clusters and/or dispersed Mo species, which are highly distorted, interacting with alumina and silica supports. X-ray photoelectron spectroscopy and diffuse reflection spectroscopy (DRS) results gave better evidence of the presence of higher amounts of Mo species at the surface of both supports when compared with the respective physical mixtures. Fourier transform infrared spectroscopy also provided good evidence that a surface reaction may have occurred between MoO₃ and hydroxyl groups on both supports. It was possible to infer that the original MoO₃ crystal lattices were destroyed by reacting with the support surface as a result of thermal treatment and transformed into small Mo clusters, dispersed Mo species, or both. Moreover, Raman spectroscopy showed nicely that the interaction of Mo species was higher on alumina than silica surfaces. Raman and DRS also provide insight into Mo species dispersion on alumina and silica samples, whereas DRS provided better evidence of the presence of dispersed Mo species on these supports. It was possible to infer that all calcined physical mixtures exhibited dispersed Mo species and small Mo clusters together with a small quantity of bulk MoO₃ that remained after thermal treatment. Therefore, similar results obtained on both supports demonstrated that the thermal spreading of MoO₃ also occurred on silica and the same mechanism was observed as on alumina. However, the Mo dispersion and some Mo species were different on the supports that can be attributed to the different surface properties of silica and alumina.

Introduction

Molybdena/alumina or molybdena/silica catalysts are very important in technological processes, such as propene metathesis,[1,2] propene oxidation,[3] methanol oxidation,[4] ethanol oxidative dehydrogenation,[1] ammonia selective oxidation to nitrogen,[5] and photochemical reactions,[6] and most important in hydrodesulfurization processes, which represent one of the largest groups in the catalytic process in the petroleum and petrochemical industries. Therefore, it is of great interest to study these types of catalysts and/or their precursors.

The usual technique of preparation is impregnation by using a heptamolybdate solution.[7–11] However, when the objective is to facilitate the formation of dispersed molybdenum species in a "monolayer" or "submonolayer", the recommended techniques are liquid-phase equilibrium adsorption[12–15] or gas-phase adsorption.[15,16] These techniques require several preparation steps and sometimes controlled atmosphere and very expensive precursors. Therefore, the preparation becomes very expensive and laborious.

Recently it has been shown that a few oxides may be dispersed spontaneously onto the surface of some oxide supports

during thermal treatment with the formation of a monolayer or submonolayer,[17] i.e., three-dimensional bulk metal oxides are transformed in two-dimensional metal oxide species on the surfaces of the oxide supports by simple thermal effect. This phenomenon, called "thermal spreading", is characterized by the dispersion over macroscopic distances of a bulk metal oxide in solid phase onto the surface of another oxide.[18–21] Thermal spreading is therefore a potential new route for preparing Mo supported catalysts. This procedure has been called clean or "friendly" because large amounts of wastewater, rejects, and additional calcination steps can be avoided.

Several researchers have reported evidence of thermal spreading phenomenon of MoO₃ onto Al₂O₃, TiO₂, SnO₂, and MgO supports.[17–24] However some researchers using mainly Raman spectroscopy have shown that thermal spreading of MoO₃ does not occur onto silica surface.[18,19] They have attributed their results to the low interaction energy between these oxides and an insignificant decrease of surface free energy of SiO₂ that, therefore, would not favor this phenomenon on silica support.

Despite this evidence, some weak evidence of thermal spreading of MoO₃ onto silica has been reported. Xie and Tang[17] observed by X-ray diffraction (XRD) a decreasing peak intensity of MoO₃ after the calcination of a mechanical mixture of MoO₃ and SiO₂, as already observed for the MoO₃–alumina system. Stampfl et al.[24] also observed this behavior on a similar Mo/SiO₂ sample and moreover a distinguished feature by laser Raman spectroscopy (Raman), with the appearance of a weak broad band at 950 cm⁻¹, which is characteristic of dispersed Mo species. Both groups correlated these observations to thermal

spreading of MoO$_3$ onto a silica surface. However, the evidence of this phenomenon on a silica support was not conclusive.

Therefore, the main focus of this work is to study the interactions that occur between MoO$_3$ and silica or alumina and by comparison to evaluate whether the thermal spreading phenomenon of MoO$_3$ on SiO$_2$ surface actually occurs.

Experimental Section

Materials. The silica and alumina supports were obtained from Degussa. The Al$_2$O$_3$ was a C-type, with 136 m^2 g^{-1}, and the SiO$_2$ an aerosil-200 with 180 m^2 g^{-1}. MoO$_3$ was obtained from Aldrich (AR grade).

Preparation Method. The supports were previously pretreated at 773 K for 4 h. The physical mixtures were prepared by hand-grinding either SiO$_2$ or Al$_2$O$_3$ and MoO$_3$ at three different support/Mo ratios (wt/wt) in an agate mortar for 10 min. These physical mixtures were then heated, raising the temperature at 10 K min^{-1} to 773 K for 24 h in a muffle furnace. The theoretical amount of Mo was calculated to get a monolayer or less on the basis of the surface area of the supports. Thus, the amount of Mo for a complete monolayer on alumina was 12 wt %, which corresponds to 11.2 μmol of Mo/m^2.[18,20,24,25] The amounts of Mo were 6 and 4 wt %, for the other samples. Similarly, for silica the amount of Mo was 6 wt % (4 μmol/m^2)[1,18,24] and for the two other samples 4 and 2 wt %. The calcined physical mixtures will be designated by x Mo/support, where x is the Mo loading. The physical mixtures were prepared with the highest Mo amount for comparison with the respective 12Mo/Al$_2$O$_3$ and 6Mo/SiO$_2$ samples. All these samples were kept in dark flasks to avoid light so that they would look predominantly white. Some calcined physical mixtures using silica became blue when exposed to light and were also characterized for comparison. This color change was not observed on the calcined physical mixtures with alumina samples.

Thermal treatment experiments of MoO$_3$ done under similar conditions as the physical mixtures did not lose weight, which means that MoO$_3$ was nonvolatilized.

Characterization. *X-ray Diffraction (XRD).* A Philips PW 1410 powder diffratometer with CuKα radiation (40 kV, 30 mA) plus a Ni filter was used with an angular range varying between 19 and 80° at 0.02° per step and 0.8 s counting per step.

Laser Raman Spectroscopy (LRS). The spectra were recorded on a Nicolet 950 FT-Raman spectrometer instrument, equipped with a nitrogen cooled Ge detector. A Nd:YAG laser (1064 nm) was used as the excitation source. The measurements were performed with a power at the sample of 100−200 mW to avoid decomposition and thermal effects. The samples were rotated to provide a noncontinuous irradiation of any given spot on the samples. The spectral slit width was typically 4 cm^{-1}.

X-ray Photoelectron Spectroscopy (XPS). A Perkin-Elmer 1257 instrument with an X-ray gun for MgKα radiation ($h\nu$ = 1253.6 eV) was used. The gun was operated at 200 W (13 kV). The step width was 0.2 eV with an integration time of 100 ms per scan and 50 scans. The spectra were referenced to the C 1s emission at 284.6 eV. The samples were disposed on a double-face tape and outgassed in a vacuum at room temperature for 1 h. They were then analyzed in the UHV (10^{-9} Torr), using an angle of 54°.

Fourier Transform Infrared Spectroscopy (FTIR). The spectra were recorded by using a Perkin-Elmer Fourier transform infrared spectrometer operating with a spectral resolution of 4 cm^{-1}. Samples were pressed into self-supporting wafers and placed in the IR cell equipped with CaF$_2$ windows. First the
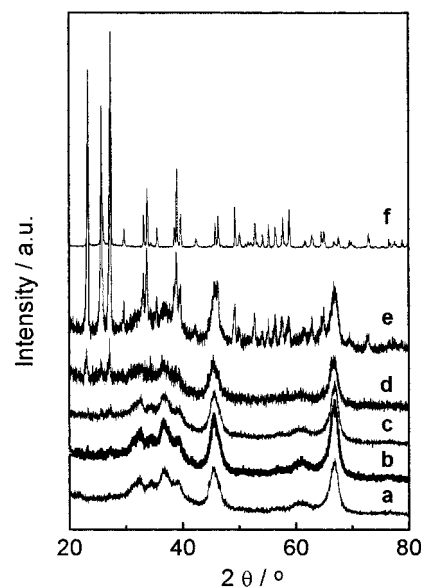

Figure 1. XDR patterns of (a) alumina support, (b) 4Mo/Al$_2$O$_3$, (c) 6Mo/Al$_2$O$_3$, (d) 12Mo/Al$_2$O$_3$, (e) the physical mixture with 12 wt % Mo, and (f) MoO$_3$. The patterns are vertically shifted and for MoO$_3$ the intensity was reduced for better visualization.

samples were submitted to pretreatment at 673 K for 1 h under conventional vacuum conditions, followed by ultrahigh vacuum at 773 K for 2 h.

Diffuse Reflection Spectroscopy (UV-DRS). These measurements were conducted in a Varian Cary 5 spectrophotometer (Harrick Scientific) with a diffuse reflectance accessory of "praying mantis" geometry and windows of silicon oxide. The samples were set in holds with 2 mm thickness. The respective Al$_2$O$_3$ or SiO$_2$ supports were used as reference compounds. The spectra were recorded in the range between 190 and 800 nm with a scanning speed of 1800 nm min^{-1}.

Results and Discussion

X-ray Diffraction (XRD). Figure 1 displays the X-ray diffraction patterns of the alumina, the physical mixture of MoO$_3$ + Al$_2$O$_3$, and the calcined physical mixtures as well as the diffraction pattern of MoO$_3$ crystalline for comparison. Pattern e shows the physical mixture exhibiting the corresponding patterns of isolated oxides. Comparing the XRD pattern of the physical mixture with that of the corresponding 12Mo/Al$_2$O$_3$ sample (pattern d) reveals that the MoO$_3$ crystalline phase was markedly reduced after the heating treatment. For samples with lower MoO$_3$ content, the crystalline phase almost vanished.

Figure 2 shows the XRD patterns of SiO$_2$, 2Mo/SiO$_2$, and 6Mo/SiO$_2$ samples (patterns b and c, respectively), as well as of the SiO$_2$ + MoO$_3$ physical mixture (pattern d) together with the MoO$_3$ (pattern e). The peaks of MoO$_3$ on the 6Mo/SiO$_2$ samples were also markedly reduced in comparison with the physical mixture pattern. This behavior was also observed on the 2Mo/SiO$_2$ sample in comparison with the corresponding physical mixture, but in this case the behavior was nearly identical to that of the silica sample, showing absence of molybdenum oxide crystalline.

We observed in both cases that the support structures did not change at all, which suggests that MoO$_3$ did not diffuse or react with alumina or silica. This result implies that it does not favor formation of other crystalline compounds.

In conclusion, these results provide evidence that after heat treatment the MoO$_3$ crystals were either transformed into very small MoO$_3$ crystals, dispersed into molybdenum species over
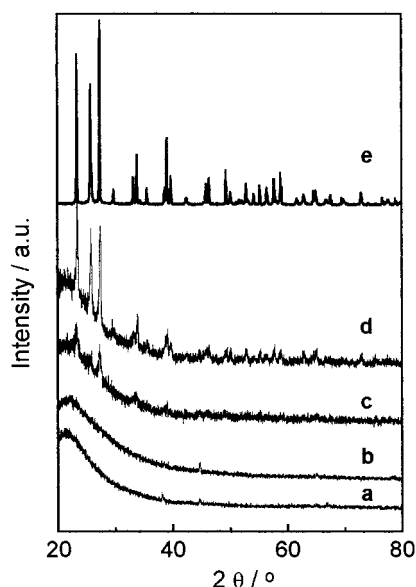
Figure 2. XDR patterns of (a) silica support, (b) 2Mo/SiO$_2$, (c) 6Mo/SiO$_2$, and (d) physical mixture with 6 wt % Mo, and (e) MoO$_3$. The patterns are vertically shifted and for MoO$_3$ the intensity was reduced for better visualization.
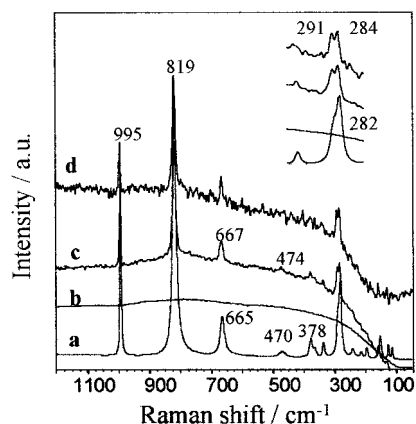

Figure 3. Laser Raman spectra of (a) MoO$_3$ crystallite, (b) alumina support, (c) physical mixture with 12% Mo, and (d) 12Mo/Al$_2$O$_3$ catalysts. The spectra were vertically shifted and the 280−290 cm^{-1} range was amplified for better visualization.

alumina and silica surfaces, or both. These results are in good agreement with the literature for alumina[17,22] and for silica systems.[24]

Laser Raman Spectroscopy (Raman). The Raman laser spectra of the 12Mo/Al$_2$O$_3$ sample (spectrum d), the corresponding Al$_2$O$_3$ + MoO$_3$ physical mixture (c), alumina (b), and MoO$_3$ (a) are shown in Figure 3. Figure 4 shows the corresponding spectra of the silica systems and MoO$_3$. Alumina did not present active modes, as reported in the literature.[26] On the other hand, SiO$_2$ exhibits a very broad and weak band in the range 480−300 cm^{-1}, as seen in Figure 4. The bulk MoO$_3$ Raman spectrum is mainly characterized by the stretching mode band of the terminal Mo=O groups at 994 cm^{-1}, the Mo−O−Mo bridge bonds at 819 and 665 cm^{-1}, and two wagging modes of the terminal Mo=O groups, i.e., the doublet at 290−280 cm^{-1}.[21]

Although the spectra of the physical mixtures show characteristic modes of the MoO$_3$ bulk, they are not strictly the sum of the corresponding support and MoO$_3$. The wavenumbers of the MoO$_3$ characteristic modes of the physical mixtures and of bulk MoO$_3$ are similar but the modes at 819 and 994 cm^{-1}
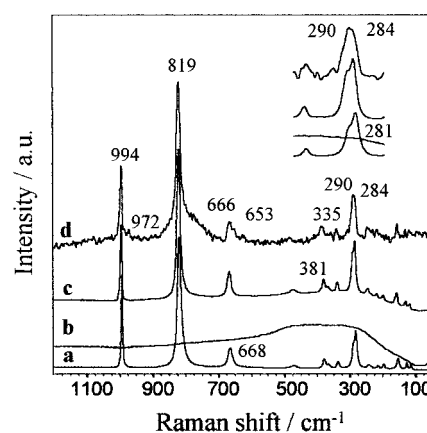

Figure 4. Laser Raman spectra of (a) MoO$_3$ crystallite, (b) the silica support, (c) the physical mixture with 6 wt % MoO$_3$, and (d) 6Mo/SiO$_2$ catalysts. Spectra were vertically shifted and the 280−290 cm^{-1} range was amplified for better visualization.

exhibited changes of the relative intensities. The intensity ratio I_{994}/I_{819} for MoO$_3$ was 0.72 but decreased to 0.49 for the MoO$_3$ + SiO$_2$ physical mixture and to 0.44 for the alumina physical mixture. This result suggests that interaction between MoO$_3$ and the supports may have occurred in the physical mixtures.

The Raman spectra of calcined physical mixtures prepared with alumina and silica showed the prevailing characteristic modes of bulk MoO$_3$. Raman spectroscopy can effectively detect the presence of small crystals and amorphous phases, which helps to identify the existence of supported compounds not detected by XRD. In addition, the Raman cross section for bulk MoO$_3$ is higher than for small Mo clusters and interaction species of Mo over alumina or over silica.[27−29] Therefore, Raman spectra will probably not show strong evidence of the Mo interaction species, depending on the amount of MoO$_3$ present in the sample. XRD results have already shown that the bulk MoO$_3$ remains in the 6Mo/SiO$_2$ and 12Mo/Al$_2$O$_3$ samples; thus, the Raman feature of the amorphous Mo species that may be formed would be overwhelmed by these small crystals. However, because the 6Mo/SiO$_2$ spectrum showed new peaks appearing at 970 and 653 cm^{-1}, compared with the physical mixture, these bands, as reported in the literature, may indicate highly dispersed surface species, probably surface molybdates[18,30,31] or polymolybdates.[10] This feature was not observed on the calcined physical mixture spectrum prepared with alumina.

Leyrer et al.[18] studied the MoO$_3$/alumina system by ISS and Kisfaludi et al.[23] by EXAFS and concluded from these techniques that thermal spreading occurred, although the Raman showed a spectrum very closely resembling the MoO$_3$. Leyrer et al.[18] interpreted this as transformation of bulk MoO$_3$ into its MoO$_4$, building up blocks onto the alumina surface as a result of the thermal treatment. Indeed, Kakuta et al.,[28] studying a Mo/SiO$_2$ system prepared by impregnation, showed by EXAFS that the major molybdenum species was different from the MoO$_3$ crystal. However, Raman results detected the presence of the MoO$_3$ crystalline phase. They interpreted these results by inferring the presence of various kinds of Mo oxide clusters on the silica support.

Apparently, although the MoO$_3$ phase remained in the calcined physical mixture, some different spectral features were observed by comparison with the physical mixtures. The main feature was that in both systems the signal/noise ratio decreased in the spectra of calcined physical mixtures, which indicated loss of intensity in the Raman spectra. This feature was more

pronounced in alumina than in silica samples. In addition, these spectra showed a small broadening band at 819 cm^{-1}. The spectra also showed change in the relative intensities of the MoO$_3$ characteristic modes at 819 and 994 cm^{-1}, although their wavenumbers were similar to those for the bulk MoO$_3$. Also the intensity ratios I_{994}/I_{819} for 6Mo/SiO$_2$ and 12Mo/Al$_2$O$_3$ sample were 0.49 and 0.44, respectively, as observed for the physical mixture. Jeziorowski et al.[32] prepared the Mo/SiO$_2$ samples by the impregnation method and observed changes in relative intensity of the peaks at 819 and 994 cm^{-1}, which were attributed to the presence of small and/or strongly distorted supported MoO$_3$ small crystals, highly dispersed and weak interaction with the support. This feature appeared on both calcined and uncalcined physical mixtures and may be interpreted as an interaction between the molybdenum oxide and the support surface as a result of the acid−base solid-state reaction, even before thermal treatment, formed during the hand-grinding and remaining unchanged after thermal treatment.

Another interesting feature in the Raman spectra of both calcined physical mixtures is the change in relative intensities of the doublet at 290−280 cm^{-1}. MoO$_3$ showed this doublet hardly resolved and the most intense peak appeared at 282 cm^{-1}. This peak remained as the most intensive in the alumina calcined physical mixture, while for silica it was at 291 cm^{-1}. On the other hand, the change of relative intensity of this doublet was also observed on the physical mixtures. Notice that for the alumina calcined physical mixture this doublet was well resolved, whereas it remained hardly resolved for the silica mixture.

The literature has reported from the vibrational spectra of powdered samples that information can be obtained not only about phases but also sizes, shapes, and states of aggregation of the particles.[33,34] Mestl et al.[35] have reported that the signal/noise ratio decreased in the spectra of the Mo/Al$_2$O$_3$ samples prepared by thermal spreading in comparison with the physical mixture and this feature was attributed to a reduction of the MoO$_3$ mean particle size as a result of the spreading phenomena. Mestl et al.[36] have shown that the change in the relative intensities of the doublet at 280−290 cm^{-1} of bulk MoO$_3$ were related to changes in the mean particle size, and when the particle size decreases the peak intensity at higher frequency of this doublet increases. Therefore, when comparing these results with ours one may conclude that the decreasing signal/noise ratio and the change in the relative intensities at the doublet at 280−290 cm^{-1} on both alumina and silica calcined physical mixtures compared with the respective physical mixtures may be correlated to the decreasing particle sizes of MoO$_3$ on both systems, i.e., the destruction of the MoO$_3$ lattice as a result of thermal treatment and, hence, spreading occurred on both supports.

The greater loss in the spectral quality and the better definition of the doublet at 280−290 cm^{-1} on the alumina calcined physical mixture as compared with the silica suggest that the dispersion of Mo species or MoO$_3$ small crystals was higher on the alumina sample.

As known, the MoO$_3$ crystallizes in the orthorhombic lattice (space group *Pbnm-D$_{26}$*) with four formula units per unit cell; its structure represents a transitional stage between octahedral and tetrahedral coordination and may be considered as being built up by MoO$_4$ tetrahedra sharing two oxygen corners with two neighboring tetrahedra to form chains running in the direction of the *c*-axis. The chains are condensed in the *a*−*c* plane to form the layered structure of MoO$_3$, and the MoO$_3$ layers are secured along the *b*-axis by van der Waals interac-
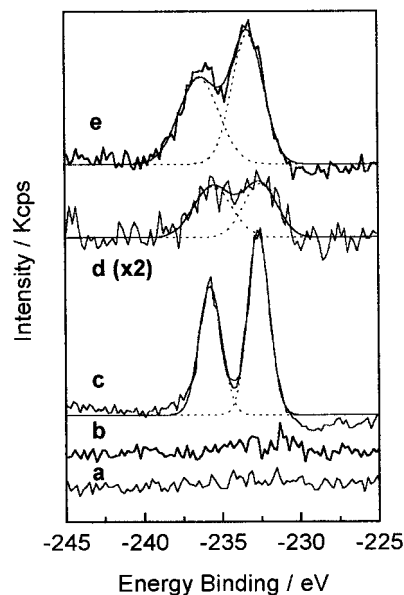

Figure 5. XPS spectra of Mo 3d region for (a) SiO$_2$ + MoO$_3$ physical mixture with 6 wt % Mo, (b) Al$_2$O$_3$ + MoO$_3$ physical mixture with 12 wt % Mo, (c) MoO$_3$, (d) 6Mo/SiO$_2$, and (e) 12Mo/Al$_2$O$_3$ catalysts. Spectra were vertically shifted for better visualization.

tions.[21] The wagging modes at 280−290 cm^{-1} of the terminal Mo=O groups are parallel polarized to the direction of the chain of tetrahedral MoO$_4$, i.e., the *c*-axis.[36] Therefore, the better resolution and change in relative intensity of this doublet may be due to the distortions along that chain by the interaction of MoO$_3$ crystals with the supports, thereby suggesting a stronger interaction between Mo species and alumina than with silica, which is in good agreement with the results reported for samples prepared by the impregnation method.[26,37]

Therefore, these changes on the spectra of calcined physical mixtures prepared with alumina and silica when compared with the respective physical mixtures show evidence of the presence of Mo species on both systems that are different from MoO$_3$ bulk. Considering similar features observed on the spectra for both calcined physical mixtures, these results may be interpreted as resulting from partial transformation of bulk MoO$_3$ in dispersed Mo species and/or even very small MoO$_3$ crystals interacting with both alumina and silica support surfaces. In addition, the peaks at 970 and 650 cm^{-1} observed on the silica calcined physical mixture spectrum indicated highly dispersed surface species, which provided additional evidence of MoO$_3$ spreading on silica support.

X-ray Photoelectron Spectroscopy. Figure 5 shows the XPS spectrum of the MoO$_3$ crystals exhibiting one characteristic doublet of a hexavalent molybdenum at 235.5 eV and 232.6 eV, which correspond to the Mo 3d$_{3/2}$ and Mo 3d$_{5/2}$ orbitals, respectively.[38] It also shows the spectra of the 12Mo/Al$_2$O$_3$ and 6Mo/SiO$_2$ samples with the corresponding physical mixtures.

The physical mixtures barely show the characteristic doublet of Mo(VI) ion because the area of the MoO$_3$ crystal when compared with the support is small and the concentration is also very low. However, these features appeared on both spectra of silica and alumina calcined physical mixtures. The Mo$_{3d}$/Al$_{2p}$ surface atomic ratio for 12Mo/Al$_2$O$_3$ sample was approximately 0.14.

The Mo$_{3d}$/Si$_{2p}$ surface atomic ratio for the physical mixture SiO$_2$ + MoO$_3$ was very small, as seen in the previous case for the alumina physical mixture. However this ratio was different for the 6Mo/SiO$_2$ sample, around 0.009. The larger the surface
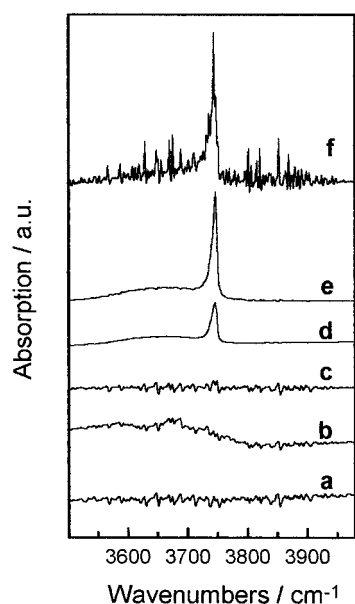
Figure 6. IR spectra of (a) 12Mo/Al_2O_3 catalyst, (b) alumina support, (c) 6Mo/SiO_2 catalyst, (d) 4Mo/SiO_2, (e) 2Mo/SiO_2, and (f) silica support.

atomic ratios for the samples, the greater the quantity of the Mo species at the surface. That is strong evidence for spreading of MoO_3 on both silica and alumina supports and in turn for the idea of transforming MoO_3 by thermal treatment into very small crystals of MoO_3 and/or into dispersed Mo species on silica and alumina surfaces.

In addition, the Mo doublet of the alumina calcined physical mixture spectrum was shifted to a higher binding energy relative to the MoO_3, exhibiting maximum peaks at 236.2 eV for Mo $3d_{3/2}$ and at 233.4 eV for Mo $3d_{5/2}$. It may be inferred as a chemical environmental change of Mo(VI) ion on the alumina sample, or as due to a decreasing mean particle size of MoO_3 due to the thermal treatment, or both.[35] This behavior could not be observed on the silica calcined physical mixture, because the signal/noise ratio was very low.

These results support spreading phenomena of MoO_3 over silica and alumina surfaces by thermal treatment and are in good agreement with previous XRD and Raman results.

Fourier Transform Infrared Spectroscopy. IR spectra of the 12Mo/Al_2O_3, 6Mo/SiO_2, 4Mo/SiO_2, and 2Mo/SiO_2 samples and the alumina and the silica supports are displayed in Figure 6. The spectrum of alumina support showed a broad band between 3500 and 3800 cm^{-1} corresponding to hydroxyl groups. However, this band was markedly reduced on the 12Mo/Al_2O_3 sample. The silica spectrum showed a narrow band around 3750 cm^{-1} for hydroxyls groups, i.e., the isolated silanol groups ($\equiv$ Si–OH). This band decreased with the MoO_3 increased on the calcined silica physical mixture. As on the 12Mo/Al_2O_3 sample, this band was also markedly reduced on the 6Mo/SiO_2 sample.

Several studies have reported that the formation of the Mo overlayer on an alumina or silica surface in Mo-supported catalysts prepared by impregnation of ammonium heptamolybdate[39,40] or other preparation methods was accompanied by a gradual consumption of free OH groups at the surface support. Therefore, our results indicated consumption of hydroxyl groups by Mo species on both systems, which confirmed a solid–solid reaction between MoO_3 and the supports and thus formation of Mo species at the surface after thermal treatment.

Diffuse Reflectance Spectroscopy. The DRS spectra of Mo/ Al_2O_3 samples and the Al_2O_3 + MoO_3 physical mixture are
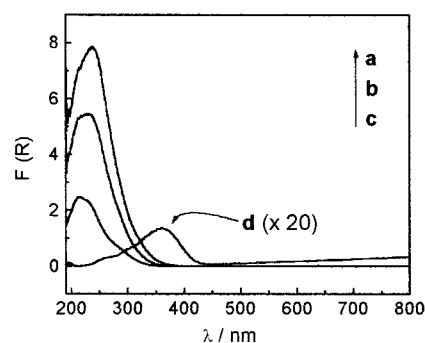

Figure 7. Diffuse reflectance spectra of (a) 12Mo/Al_2O_3, (b) 6Mo/ Al_2O_3, (c) 4Mo/Al_2O_3, and (d) the physical mixture Al_2O_3 + MoO_3 with 12 wt % Mo.
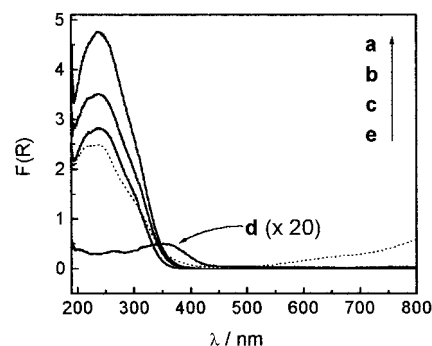

Figure 8. Diffuse reflectance spectra of (a) 6Mo/SiO_2, (b) 4Mo/SiO_2, (c) 2Mo/SiO_2, (d) the physical mixture SiO_2 + MoO_3 with 6 wt % Mo, and (e) the 2Mo/SiO_2 after exposure to the atmosphere for more than 1 week.

shown in Figure 7, while Figure 8 shows the spectra of the Mo/SiO_2 samples and the corresponding SiO_2 + MoO_3 physical mixture. All the calcined physical mixtures showed only one absorption band in the UV–visible range of the electronic spectra, which corresponds to an Mo(VI) ion with a d^0 electronic configuration. This valence–conduction band transition was attributed to the ligand–metal charge transfer (LMCT): O^{2-} $\rightarrow$ Mo^{6+}, usually observed between 200 and 400 nm. The valence band is generated by an oxygen $2p\pi$-orbital, while the conduction band is generated by overlapping metal 4d and 5s orbitals.

When these systems were compared with the corresponding physical mixture, two main features were observed: the absorption bands were shifted to lower wavelengths and the intensities were higher. The UV diffuse reflectance spectrum may distinguish a dispersed monolayer from a crystalline oxide or salt by the absorption intensity spectra. The intensity of dispersed monolayer or submonolayer increases markedly compared with crystalline materials as a result of the multiple reflection effects between light and dispersed species.[17,41] One can conclude, from the higher absorption band intensities observed on the calcined physical mixtures compared with the respective physical mixture, that dispersed Mo species are present on the alumina and silica surfaces. Moreover, the increasing absorption band intensities with the molybdenum amount in the calcined physical mixtures may be related to the increasing formation of Mo species at these surfaces.

Comparing the spectra of alumina and silica calcined physical mixtures reveals that the silica samples exhibited absorption bands shifted to higher wavelengths than the alumina samples. All the silica calcined physical mixtures showed one band around 238 nm. However, the alumina samples showed bands ranging from 215 to 240 nm (Figure 7). Noteworthy is that the

widths of the Mo/SiO$_2$ bands are larger than on alumina samples, with a shoulder at higher wavelengths. Both physical mixtures showed one band at 360 nm, but the Al$_2$O$_3$ + MoO$_3$ physical mixture showed an additional broad band at higher wavelengths.

The DRS band position strongly depends on structural factors, like the interactions between Mo and the support and/or dispersion of Mo. Indeed, Fournier et al.[42] observed that Mo clusters size and distance between clusters have much more influence than local Mo symmetry. Moreover, they observed a broadening and a shifted band toward higher wavelength for the lowest energy absorption band when cluster sizes increased and, in contrast, a narrowing and blue-shift band for increasing Mo dispersion. Weber[43] proposed an empirical correlation between the optical band gap energy of the DRS spectra and the average number of adjacent molybdenum ions in very small oxide clusters. In this correlation, better represented by the energy of the absorption edge, the position of the absorption edge was determined by finding the interception of a straight line fitted through the low energy rise in the plots of $[F(R)h\nu]^2$ vs $h\nu$. Thus, the DRS spectrum was transformed from $F(R)$ vs λ to $[F(R)h\nu]^2$ vs $h\nu$ (where $F(R)$ is the Kubelka–Munk function and $h\nu$ is the energy of incident photon in electronvolts. According to this method,[43] the greater the edge energy, the lesser the number of the next nearest neighbors. Energy values around 2.7 eV are referred to as $[Mo_6O_{19}]^{2-}$ polyanions; for MoO$_3$ and polyanions such as $[Mo_7O_{24}]^{6-}$, $[Mo_2O_7]^{2-}$, $[MoO_4]^{2-}$, the values were 3.0, 3.3, 3.9, and 4.3 eV, respectively. The condensation degree decreased in that sequence. Therefore, with this correlation, it was possible to infer prevailing neighboring Mo in the calcined physical mixtures. The energy values obtained were 4.2 eV for all Mo/alumina and 3.8 eV for Mo/silica samples. One can conclude that the Mo species were highly dispersed on both supports, but the dispersion was higher on alumina than on silica, attributed to the $[MoO_4]^{2-}$ polyanion on alumina and $[Mo_2O_7]^{2-}$ on silica. These results agree with those of Fournier et al.[42]

Comparison between the shift band positions of 12Mo/Al$_2$O$_3$ and 6Mo/SiO$_2$ samples with the respective physical mixtures can be related to the condensation degree of these Mo species, which may be assigned as the transformation of MoO$_3$ to Mo dispersed species or MoO$_3$ microcrystals and, therefore, to the occurrence of MoO$_3$ spreading onto these supports. Moreover, one can conclude that the support affects the Mo species dispersion.

Independent of the variation of the band position on alumina calcined physical mixtures with the molybdenum amount, the energy of the absorption edge was the same, reinforcing the high dispersion statement, which can be related to the closer proximity of Mo species for higher Mo amounts attributed to the density of high OH groups on alumina.

Comparing the spectra of physical mixtures reveals the appearance of a broad band above 500 nm in the spectrum of the Al$_2$O$_3$ + MoO$_3$ physical mixture that was not present in the spectrum of the silica mixture. This broad band may be correlated to the presence of substoichiometric molybdenum oxide (MoO$_{3-X}$), i.e., the defect structures, and can be assigned to polaron conductance (Mo^{5+}–O–Mo^{6+} intervalence transfer) known for molybdenum suboxides. It is known that MoO$_3$ exhibits an intrinsic variability in the oxygen content and a whole series of ordered defect structures in the range between MoO$_3$ and MoO$_2$. Mestl et al.[44] have shown that the presence of defects in the MoO$_3$ crystal lattice may be reflected in the electronic spectra. One may think that this feature would correlate to the hand-grinding, where the physicochemical

properties, such as composition, structure, particle morphologies, porosity, interatomic distances, lattice symmetries, etc., of MoO$_3$ would be changed by the mechanical stress applied during this process. However, this is not true because this band is absent in the spectrum of the SiO$_2$ + MoO$_3$ physical mixture. Therefore, this spectral feature may be correlated with a different interaction between MoO$_3$ and the supports favored only by hand-grinding. This interaction may reduce Mo^{6+} of MoO$_3$ to Mo^{5+} ions, and these Mo^{5+} centers, through Mo^{5+}–O–Mo^{6+} interactions, form an additional conduction band. These results as much as the Raman ones provide evidence of the stronger interaction between MoO$_3$ and alumina even in physical mixture after the hand-grinding than between MoO$_3$ and silica.

The DRS spectra of the fresh 2Mo/SiO$_2$ sample (curve c) and that after exposure to the atmosphere for more than 1 week (curve e), which was blue as described above, are shown in Figure 8. After exposure to the atmosphere a broad band around 700–750 nm appeared, characteristic of molybdenum blues that are actually blue. The molybdenum blues are mixed-valence compounds and the blue color arises presumably from the intervalence Mo$^{5+} \rightarrow$ Mo^{6+} or Mo^{5+}–O–Mo^{6+} electronic transition, which can be viewed as intermediate species of mixed oxyhydroxides.[45,46] The blue color of this sample, therefore, indicates the presence of Mo(V) ion on the silica calcined physical mixture, which occurs after the exposure to light that originated the broad band around 700 nm. Thus, clearly dispersed Mo species were formed on silica supports by thermal treatment that may be transformed to Mo species containing Mo(V). These results provide additional evidence for the MoO$_3$ spreading phenomenon onto silica surfaces.

It has been suggested that spreading of MoO$_3$ is an exfoliation process because this oxide cleaves relatively easily parallel to the (010) and (100) layers.[18] Our results indicated that thermal treatment of a physical mixture of MoO$_3$ and silica or alumina induced this spreading phenomenon, transforming partially the MoO$_3$ crystals into small Mo clusters and dispersed Mo species. Although a microscopic explanation of the spreading phenomenon is not possible yet, we claim that an exfoliation process may really happen, where faces of MoO$_3$ crystals initially react with hydroxyl groups of the supports, favoring cleavage of adjacent layers or cleavage of neighbor layers with point defects, like vacancies, interstitial ions, etc. Therefore, the original MoO$_3$ crystals were broken during thermal treatment into smaller crystals, reacting then with other hydroxyl groups, and so on. This process dispersed Mo species together with very small Mo clusters. The MoO$_3$ bulk that remained even after thermal treatment may be attributed to the kinetics of spreading as well as sintering or crystal grow in MoO$_3$ agglomerates due to thermal activation. It is noteworthy that similar results were obtained for silica and alumina supports and thus the same mechanism occurred with both supports.

In comparing DRS and Raman results for alumina and silica calcined physical mixtures, we note not only the blue color of the silica sample exposed to the atmosphere but also that the nature of the support influences strongly the interaction with the molybdenum oxide phase, and the strength of this interaction determines for the Mo species formation. DRS results exhibited Mo species on alumina that resembles MoO$_4^-$ ions, whereas on silica the species mainly resembles Mo$_2$O$_7^{2-}$. These species may be correlated to the formation of dispersed Mo species by thermal spreading of MoO$_3$. Considering that the destruction of the MoO$_3$ crystal lattice occurs during the reaction between the oxides, probably MoO$_4$ units of MoO$_3$ bulk phase are dispersed on alumina to form the dioxomolybdenum(VI) species,

whereas on silica calcined physical mixtures, the species might be associated with dimeric molybdenum oxide ones;[48] however, the formation of these species is controversial.[49]

The literature reports that the amount of MoO_3 needed for a theoretical monolayer coverage on SiO_2 supported molybdenum by the impregnation method is smaller than that on alumina as a result of the weaker interaction of MoO_3 with silica than with alumina.[26] This may be attributed to a different basicity of the silanol and the OH groups on alumina. A general acid−base reaction may represent the interaction of molybdenum oxide with the support. The facts that alumina in solid phase and in the absence of water is amphoteric and silica is approximately neutral, whereas MoO_3 is a weak acid, would explain the weaker interaction between MoO_3 and silica. In addition, alumina presents higher OH group density than silica, as shown by IR, and thus higher accessibility of MoO_3 to the hydroxyl groups of alumina. Thus, during the thermal treatment of the physical mixture of $SiO_2 + MoO_3$, as a result of the high local amount of MoO_3 crystals, the low density of silanol groups and the weak interaction between these oxides explain the low dispersion of MoO_3 onto the silica surface.

References and Notes

(1) Ono, T.; Anpo, M.; Kubokawa, Y. *J. Phys. Chem.* **1986**, *90*, 4780.
(2) Liu, T.-C.; Forissier, M.; Coudurier, G.; Védrine, J. C. *J. Chem. Soc., Faraday Trans. 1* **1989**, *85*, 1607.
(3) Giordano, N.; Meazzo, M.; Castellan, A.; Bart, J. C.; Ragaini, V. *J. Catal.* **1997**, *50*, 342.
(4) Louis, C.; Tatibouët, J. M.; Che, M. *J. Catal.* **1988**, *109*, 354.
(5) de Boer, M.; van Dillen, A. J.; Koningsberger, D. C.; Geus, J. W.; Vuurman, M. A.; Wachs, I. E. *Catal. Lett.* **1991**, *11*, 227.
(6) Yang, T.-J.; Lunsford, J. H. *J. Catal.* **1987**, *103*, 55.
(7) Cheng, C. P.; Schrader, G. L. *J. Catal.* **1979**, *60*, 276.
(8) Cheng, C. P.; Ludowise, J. D.; Schrader, G. L. *Appl. Spectrosc.* **1980**, *34*, 146.
(9) Ng, K. Y. S.; Gulari, E. *J. Catal.* **1985**, *92*, 340.
(10) Jeziorowski, H.; Knözinger, H. *J. Phys. Chem.* **1979**, *83*, 1166.
(11) Liu, Y. C.; Griffin, G. L.; Chan, S. S.; Wachs, I. E. *J. Catal.* **1985**, *94*, 108.
(12) Chan, S. S.; Wachs, I. E.; Murrel, L. L.; Wang, L.; Hall, W. K. *J. Phys. Chem.* **1984**, *88*, 5831.
(13) Suarez, W.; Dumesic, J. A.; Hill, C. G., Jr. *J. Catal.* **1985**, *94*, 408.
(14) Wang, L.; Hall, W. K. *J. Catal.* **1980**, *66*, 251.

(15) Wang, L.; Hall, W. K. *J. Catal.* **1983**, *83*, 242.
(16) Sonnemans, J.; Mars, P. *J. Catal.* **1973**, *31*, 209.
(17) Xie, Y.-C.; Tang, Y.-Q. *Adv. Catal.* **1990**, *37*, 1.
(18) Leyrer, J.; Margraf, R.; Taglauer, E.; Knözinger, H. *Surf. Sci.* **1988**, *201*, 603.
(19) Leyrer, J.; Mey, D.; Knözinger, H. *J. Catal.* **1990**, *124*, 349.
(20) Margraf, R.; Leyrer, J.; Taglauer, E.; Knözinger, H. *Surf. Sci.* **1987**, *189/190*, 842.
(21) Mestl, G.; Srinivasan, T. K. K. *Catal. Rev.−Sci. Eng.* **1998**, *40*, 451.
(22) Mahipal Reddy, B.; Padmanabha Reddy, E.; Srinivas, S. T. *J. Catal.* **1992**, *136*, 50.
(23) Kisfaludi, G.; Leyrer, J.; Knözinger, H.; Prins, R. *J. Catal.* **1991**, *130*, 192.
(24) Stampfl, S. R.; Chen, Y.; Dumesic, J. A.; Niu, C.; Hill, C. G., Jr. *J. Catal.* **1987**, *105*, 445.
(25) Leyrer, J.; Zaki, M. I.; Knözinger, H. *J. Phys. Chem.* **1986**, *90*, 4775.
(26) Desikan, A. N.; Huang, L.; Oyama, S. T. *J. Chem. Soc., Faraday Trans.* **1992**, *88*, 3357.
(27) Zingg, D. S.; Makovsky, L. E.; Tischer, R. E.; Brown, F. R.; Hercules, D. M. *J. Phys. Chem.* **1980**, *84*, 2988.
(28) Kakuta, N.; Tohji, K.; Udagawa, Y. *J. Phys. Chem.* **1988**, *92*, 2583.
(29) Baltrus, J. P.; Makovsky, L. E.; Stencel, J. M.; Hercules, D. M. *Anal. Chem.* **1985**, *57*, 2500.
(30) Margraf, R.; Leyrer, J.; Taglauer, E.; Knözinger, H. *React. Kinet. Catal. Lett.* **1987**, *35*, 261.
(31) Machej, T.; Haber, J.; Turek, A. M.; Wachs, I. E. *Appl. Catal.* **1991**, *70*, 115.
(32) Jeziorowski, H.; Knözinger, H.; Grange, P.; Gajardo, P. *J. Phys. Chem.* **1980**, *84*, 1825.
(33) Genzel, L.; Martin, T. P. *Surf. Sci.* **1973**, *34*, 33.
(34) Graham, G. W.; Weber, W. H.; Peters, C. R.; Usman, R. *J. Catal.* **1991**, *130*, 310.
(35) Mestl, G.; Verbruggen, N. F. D.; Lange, F. C.; Tesche, B.; Knözinger, H. *Langmuir* **1996**, *12*, 1817.
(36) Mestl, G.; Srinivasan, T. K. K.; Knözinger, H. *Langmuir* **1995**, *11*, 3795.
(37) Desikan, A. N.; Huang, L.; Oyama, S. T. *J. Phys. Chem.* **1991**, *95*, 10050.
(38) Wagner, C. D.; Riggs, W. M.; Davis, L. E.; Moulder, J. F. In *Handbook of X-ray photoelectron spectroscopy*; Muilenberg, G. E., Ed.; Perkin-Elmer: Eden Prairie, MN, 1979.
(39) Topsøe, N.; Topsøe, H. *J. Catal.* **1993**, *139*, 631.
(40) Vít, Z.; Zdrazil, M. *J. Catal.* **1997**, *171*, 305.
(41) Lipsch, J. M. J. G.; Schuit, G. C. A. *J. Catal.* **1969**, *15*, 174.
(42) Fournier, M.; Louis, C.; Che, M.; Chaquin, P.; Masure, D. *J. Catal.* **1989**, *119*, 400.
(43) Weber, R. *J. Catal.* **1995**, *151*, 470.
(44) Mestl, G.; Verbruggen, N. F. D.; Knözinger, H. *Langmuir* **1995**, *11*, 3035.
(45) Bucley, R. I.; Clark, R. J. H. *Coord. Chem. Rev.* **1985**, *65*, 167.
(46) Yamase, T. *J. Chem Soc., Dalton Trans.* **1982**, 1987.
(47) Iwasawa, Y.; Ogasawara, S. *J. Chem. Soc., Faraday Trans. 1* **1979**, *75*, 1465.
(48) Iwasawa, Y. *Adv. Catal.* **1987**, *35*, 187.
(49) Kikutani Y. *J. Mol. Catal. A: Chem.* **1999**, *142*, 247.